A PRESSURE SENSOR ARRAY WITH SENSING RANGES TUNABLE BY DRIVING FREQUENCY

Yu-Tse Lai and Yao-Joe Yang
National Taiwan University, Taipei, TAIWAN

ABSTRACT

This work presents the development of a novel 4×4 pressure sensing array with tunable sensing ranges. Carbon nanotubes (CNTs) dispersed in nematic liquid crystals (LC) composite is employed as the resistive sensing material. The structure of the sensing element, in which the LC-CNT composite is sealed, consists of a deformable PDMS elastomeric structure, an indium tin oxide (ITO) glass substrate and an ITO PET film. The force sensing ranges can be tuned by varying frequency of the driving voltage supplied by the array scanning circuitry. This tunable capability can be employed for the applications which require different measurement ranges of forces, without the need of adjusting the dynamic ranges of the sensor readout circuitry. The characteristics of the devices are measured and the pressure images with tunable capability are successfully captured. The driving and scanning circuit for resistive sensing array is also designed and implemented.

1 INTRODUCTION

Tactile sensing arrays are essential for robots to detect physical contact with humans or environment. Many researches on sensor arrays for normal and shear force detection have been reported. The typical sensing mechanisms for tactile arrays include capacitive [1], resistive [2], piezoelectric [3], and optical [4]. In addition, many other research works have been focused on manufacturing techniques, reliability issues, or special sensing functionalities. For example, an innovative approach has been proposed to realize a highly twistable and reliable artificial skin by using spiral electrodes as sensing electrodes and scanning traces [5]. Bao et al. [6] demonstrated flexible capacitive pressure sensors with excellent sensitivity and short response times that can be inexpensively fabricated over a large area by patterning thin films of a biocompatible PDMS polymer.

The study on carbon nanotubes (CNTs) dispersed in nematic liquid crystals (LC) has received attentions recently [7]. It has been observed that the LC media can be strongly anchored to the CNT surface [8]. Also, the orientational order of LC can be transmitted to CNTs, which in turn gives rise to a high level of nematic order in CNTs organization. The electrical state of the LC-CNT composite can be switched between insulating and conducting states by varying the molecular orientation of the LC and CNT entities with external electric fields [9]. Also, it has been observed that the conductivity of LC-CNT composites is dependent on certain physical parameters, such as the concentrations of CNTs [10], temperature [10-11], electric (and magnetic) field [12-13], and frequency [13].

In this work, by employing LC-CNT composite and micromachining techniques, we first report a tactile sensing array which possesses the capability of tunable sensing ranges. The structure of the sensing element, in which the LC-CNT composite is sealed, consists of a deformable PDMS elastomeric structure, an indium tin oxide (ITO) glass substrate, and an ITO PET film. The 4×4 electrode patterns on the ITO film and ITO substrate are fabricated by using typical lithography and etching techniques. The force sensing ranges can be tuned by varying the driving frequency for LC-CNT composites. The corresponding driving and scanning circuit is designed and developed. The characteristic of the sensing material and the performance of the sensing array will be measured and discussed.

2 DESIGN

The frequency dependence of electrical conductivity for LC-CNT composites has been reported in [14]. Higher driving frequency of LC-CNT composites induces higher conductivity (i.e., lower resistivity). In addition, similar to conductive polymers [15], LC-CNT composites also exhibit resistance change under external pressure forces. In this work, we utilize these behaviors to design and develop tactile sensing devices with tunable force sensing ranges. Fig. 1(a) shows the schematic of the proposed device. The upper and lower layers of the device are a PET film and a glass substrate, respectively. The PET film and the glass substrate are coated with ITO on one side. The deformable spacer layer is a PDMS polymer film. The sensing material is made by dispersing multi-walled CNTs (MWCNTs) in nematic liquid crystal (NLC) medium. The size of the 4×4 sensing array is $20\ mm \times 20\ mm$, and the size of each sensing element is $2\ mm \times 2\ mm$. The width of the metal trace between each element is $100\ \mu m$. Fig. 1(b) shows the cross-sectional view of an element. The LC-CNT mixtures are sandwiched between an ITO PET film and an ITO glass. The thicknesses of the PET film, the PDMS layer and the glass substrate are $100\ \mu m$, $500\ \mu m$ and $700\ \mu m$, respectively.

3 FABRICATION

The liquid crystal (E7, Merck, Taiwan) used in this work has a nematic phase at room temperature, and its clearing point is 59.6 $^{\circ}C$ (i.e, N-I phase transition

temperature, T_{NI}) The MWCNTs used for this work are 10~20 nm in diameter and 1~2 μm in length with 95% purity. The MWCNTs were doped at a fixed concentration of 0.5 wt% in the LC material (E7) and subjected to ultrasound at 40 kHz (400W) with 70 $°C$ for 5 hours to reduce the CNTs bundling tendency. Finally, the mixture was degassed and the composite preparation was finished.

Fig. 2 illustrates the fabrication process for the sensing array. Fig. 2(a) shows the fabrication processes for the upper and the lower electrode layers. The ITO glass and the ITO PET film, which are commercially available, were diced into smaller pieces of 20 $mm \times 20\ mm$. Then, the ITO electrode structures on the PET film were patterned by oxalic acid with photoresist as etching masks. Similar patterning process was also used to create the ITO electrode patterns on the glass substrate. Fig. 2(b) is the fabrication process of the PDMS structure layer. PDMS prepolymer and curing agent (Sylgard® 184A and 184 B, Dow Corning) are mixed at a 10:1 ratio. After stirred thoroughly and degassed in a vacuum chamber, the prepared PDMS mixture was poured onto a patterned SU-8 master (GM 1070, Gersteltec Sarl). After cured at 90 $°C$ for 60 minutes, the cured PDMS layer was peeled from the master substrate. Fig. 2(c) is the schematic of the assembled device. The lower ITO glass and the PDMS layer were bonded together after oxygen plasma treatment. Again, after oxygen plasma treatment on the top of the PDMS layer, the prepared LC-CNT composite was injected in the cell by a syringe, and then the upper ITO PET was bonded on the PDMS layer. The fabricated components and the assembled device are shown in Fig. 3. Fig. 3(a) shows the electrode pattern on the ITO glass. The upper electrode patterns on the flexible ITO PET are shown in Fig. 3(b). Fig. 3(c) and 3(d) show the pictures of the fabricated 4×4 tactile sensing array.

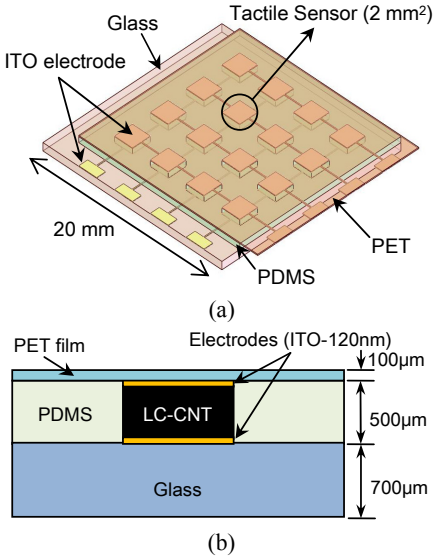

Fig. 1. (a) The schematic of the proposed sensing array (b) The detailed illustration of the tactile sensing element.

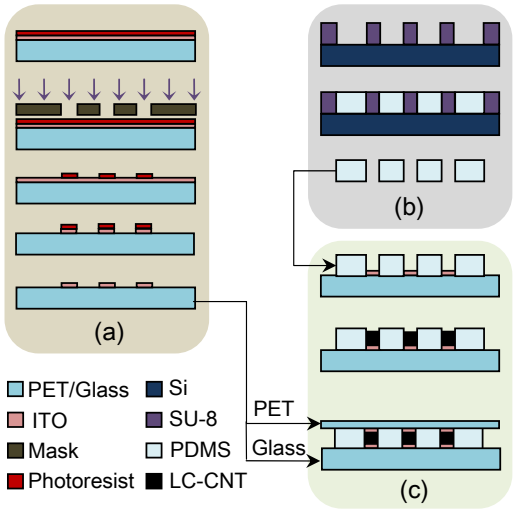

Fig. 2. The fabrication processes of the proposed sensor module: (a) The ITO electrode layer, (b) The PDMS structure layer, (c) The assembled device.

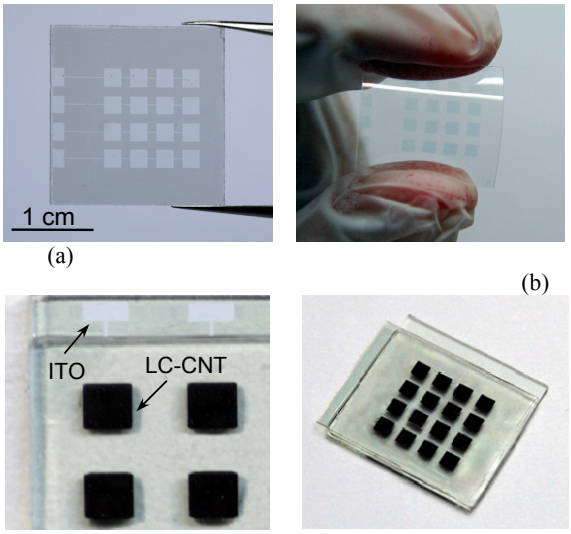

Fig. 3. (a) The lower electrodes on a ITO glass substrate. (b) The upper electrodes on a ITO PET film. (c) The fabricated sensing element. (d) The fabricated 4×4 tactile sensing array.

4 MEASUREMENT AND DISCUSSION

Fig. 4 is the experimental setup for measuring the proposed sensor element. A force gauge (HF-5, ALGOL) is used to measure the applied force. The force gauge is fixed on a z-axis (vertical) translational stage whose displacement resolution is 1 μm. The cell is then sandwiched by a metal plate and a metal probe. Resistance measurements were

performed using an LCR meter (Wayne Kerr, 6440A) which is capable of providing a large oscillating voltage (up to 10 V_{rms}) with a frequency range from 20Hz to 3MHz. Fig. 5 shows the measured curves of resistance vs. frequency of the sensing element. Under different driving voltages, the resistance decreases as the frequency increases. The threshold voltage of E7 is about 1.08V. Therefore, the curves with driving voltages of 0.1V and 1V are almost the same since both of the driving voltages are insufficient to reorient the LC molecules and CNTs.

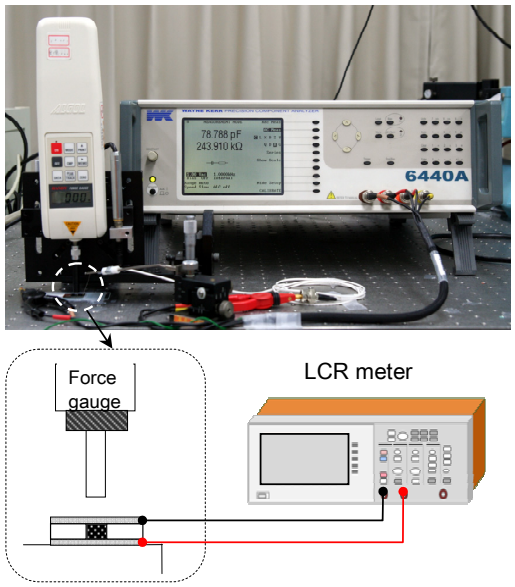

Fig. 4. Experimental setup for measuring the resistance of the LC-CNT sensing element.

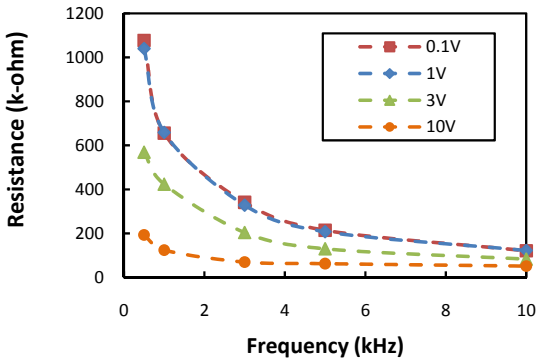

Fig. 5. The resistance versus frequency plots for different driving voltage.

The measured relationships of resistance versus applied pressure for the sensing elements under different frequencies are shown in Fig. 6. In this experiment, the external pressure increases from 0 to 250 kPa. The driving voltage is fixed on 3V. Three different frequencies (1kHz, 3kHz and 5kHz) are applied to the device. The resistances decrease as the applied pressures increase. However, for each curve, the resistance approaches to a minimum (about 30 $k\Omega$) as the applied pressure is greater than certain value. Based on the behavior shown in this figure, within the same resistance variation range, different force sensing ranges can be obtained by changing the driving frequency. This characteristic can be adopted for the pressure sensing devices with tunable sensing ranges, without the need of adjusting the dynamic ranges of the sensor readout circuitry.

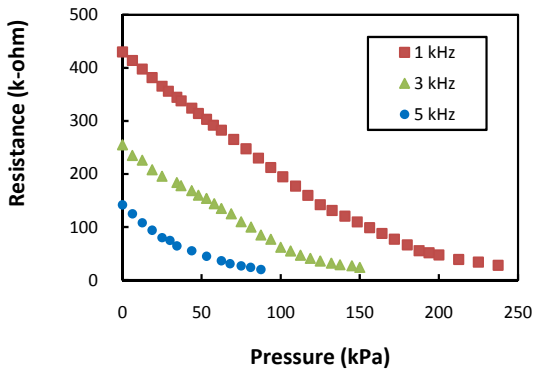

Fig. 6. Measured responses of the fabricated tactile sensing element at different frequencies.

Fig. 7 is the picture of the experimental setup. The measured array sensing images are shown in Fig. 8. The applied pressure increases gradually from 0 kPa to 200 kPa. At certain driving frequency, as the applied pressure is out of the force sensing range for the read-out circuit, will be out of the dynamic range of the ADC. Then, the frequency can be changed so that can be shifted back to the dynamic range. The force images under different frequencies (5kHz, 3kHz, 1kHz) are shown in Fig. 8(a), 8(b) and 8(c). The applied pressures for Fig. 8(a-ii), (b-ii) and (c-ii) are quite different. However, with capability of tuning sensing ranges by frequencies, the resistance variations are within the similar dynamic ranges for the read-out circuit.

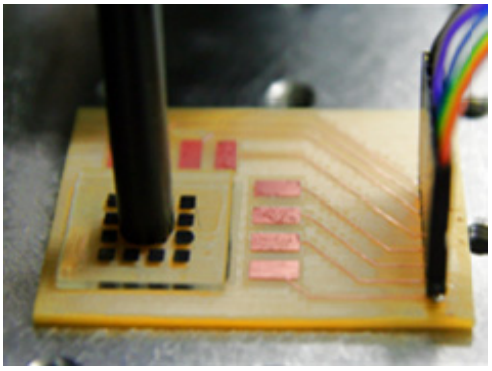

Fig. 7. Experimental setup for sensing array.

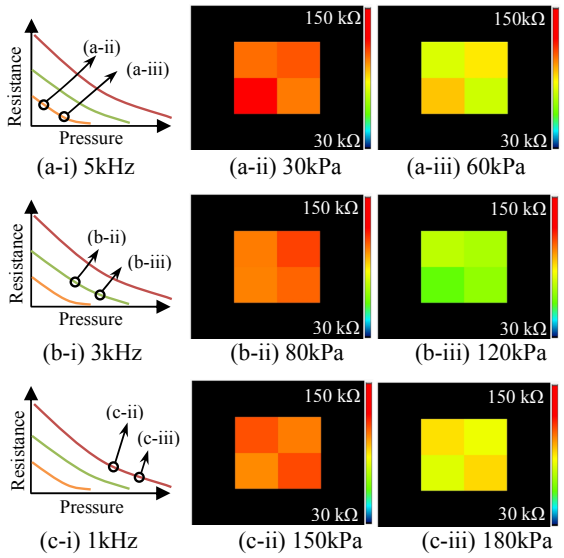

Fig. 8. Force images of a 4×4 sensing array at different frequencies. (a) Force images at 5kHz (b) Force images at 3kHz. (c) Force images at 1kHz.

5 CONCLUSION

A novel 4×4 pressure sensing array with tunable sensing ranges was presented in this paper. Carbon nanotubes dispersed in nematic liquid crystals composites were employed as the sensing material. The sensing array consists of the proposed sensing material, a deformable PDMS elastomeric structure, an ITO glass substrate and an ITO PET film. The sensing ranges are tunable by varying the driving frequency. This capability of tunable sensing ranges can be employed for the applications which require different measurement ranges of forces, without the need of adjusting the dynamic ranges of sensor readout circuitry. The tunable characteristics were measured and discussed. The corresponding scanning circuit for the sensing array was designed and implemented. Using a 4×4 sensing array, force images at different frequency and pressure were also demonstrated.

ACKNOWLEDGEMENT

This project is partially sponsored by the National Science Council, Taiwan. (Contract number: NSC 97-2628-E-002 -049 -MY3).

REFERENCES

[1] H.K. Lee, J. Chung, S.I. Chang, E. Yoon , Journal of microelectromechanical systems, 17 (2008), 934-942.
[2] Y.J. Yang, M.Y. Cheng, W.Y. Chang, L.C. Tsao, S.A. Yang, W.P. Shih, F.Y. Chang, S.H. Chang, K.C. Fan, Sensors and actuators A, 143 (2008), 143-153.
[3] J. Yoo, J. Hong, H. Lee, Y. Jeong, B. Lee, H. Songa, J. Kwon, Sensors and Actuators A, 126 (2006), 41-47.
[4] M. Rothmaier, M.P. Luong, F. Clemens, Sensors, 8 (2008), 4318-4329.
[5] M.Y. Cheng, C.M. Tsao, Y.Z. Lai, Y.J. Yang, Sensors and actuators A, 166 (2011), 226-233.
[6] S.C.B. Mannsfeld, B.C.K. Tee, R.M. Stoltenberg, C.V.H.H. Chen, S. Barman, B.V.O. Muir, A.N. Sokolov, C. Reese, Z. Bao, Nature materials, 9 (2010), 859-864.
[7] M.D. Lynch, D.L. Patrick, Organizing Carbon Nanotubes with Liquid Crystals, Nano letters, 2 (2002), 1197-1201.
[8] R. Basu and G.S. Iannacchione, Applied physics letters, 95 (2009), 173113.
[9] I. Dierking, G. Scalia, P. Morales, D. LeClere, Advanced materials, 11 (2004), 865-869.
[10] N. Lebovka, T. Dadakova, L. Lysetskiy, O. Melezhyk, G. Puchkovska, T. Gavrilko, J. Baran, M. Drozd, Journal of molecular structure, 887 (2008), 135-143.
[11] A.I. Goncharuk, N.I. Lebovka, L.N. Lisetski, S.S. Minenko, Journal of physics D, 42 (2009), 165411.
[12] V. Jayalakshmi, S. Krishna Prasad, Applied physics letters, 94 (2009), 202106.
[13] I. Dierking, S.E. San, Applied physics letters, 87 (2005), 233507.
[14] L. Dolgov, O. Kovalchuk, N. Lebovka, S. Tomylko, O. Yaroshchuk, Carbon nanotubes (2010), Jose Mauricio Marulanda (Ed.), ISBN: 978-953-307-054-4.
[15] T. Sekitani, Y. Noguchi, K. Hata, T. Fukushima, T. Aida, T. Someya, Science, 321 (2008), 1468-1472.